The formation of an intense filament controlled by interference of ultraviolet femtosecond pulses

Yongdong Wang, Yisan Zhang, Peng Chen, Liping Shi, Xin Lu, Jian Wu, Liang'en Ding,[a] and Heping Zeng

State Key Laboratory of Precision Spectroscopy, East China Normal University, Shanghai 200062, People's Republic of China

(Received 7 December 2010; accepted 21 February 2011; published online 14 March 2011)

We experimentally investigated the formation of a wavelength-scale photonic plasma grating induced by interference-assisted coalescence of two noncollinear ultraviolet femtosecond laser pulses. The period of the created plasma grating decreased with the crossing angle of the interacting laser pulses. For a proper small crossing angle, the noncollinear ultraviolet filaments were coalesced and an intense single ultraviolet filament was formed with a diameter of 5 μm which was below the focused limitation. This may provide a way to control ultraviolet femtosecond filamentation. © *2011 American Institute of Physics*. [doi:10.1063/1.3565158]

Due to its abundant nonlinear optical effects and extensive applications, femtosecond (fs) laser induced filamentation in infrared (IR) spectral region has attracted considerable interest, and a lot of interesting phenomena, such as self-focusing, self-channeling, self-phase modulation, and spectral broadening,[1,2] have been observed.[1–4] The ultraviolet (UV) fs laser pulse has numerous outstanding optical features, such as excellent focus ability, high photon energy, large ionization rate, and so forth.[1] It is nevertheless somehow difficult to generate high-intensity UV fs pulses, and due to the lack of suitable UV fs sources, researches on UV fs filaments are not so prevailing as those on near-IR filaments.

On the other hand, interaction of multiple filaments was demonstrated to be much more interesting and has led to many applications, including intense light kick,[5,6] third-harmonic[7] and THz (Ref. 8) enhancement, filamentation dynamics control,[9] white-light generation,[10] and periodic filament arrays formation.[11] By coupling two spatiotemporally overlapped noncollinear near-IR filaments, plasma waveguide arrays[12,13] were demonstrated and showed a lot of interesting effects, such as energy exchange[14,15] and plasma density modulation.[16]

In this letter, by controlling the interaction of two noncollinearly overlapped UV fs filaments, we demonstrated interference-assisted coalescence of two UV fs filaments. Wavelength-scale photonic plasma grating was formed along the interference fringes of the two overlapping UV fs pulses. The period of the created plasma grating was closely dependent on the crossing angle and more interestingly, an intense single UV filament could be resulted for two UV fs filaments overlapped at a small crossing angle. The modulated intensity distribution in the coalesced plasma channel was constructed directly by measuring the ionic fluorescence. It is well-known that filamentation is accompanied with multiphoton ionization and high order nonlinear effects which limit the guided peak intensities in the filament channels,[1] and that plasma density in filaments could not increase with the input laser energy due to the intensity clamping effects.[17] Until recently, filamentation without intensity clamping was observed by Kiran *et al.*[18] The observed coalescence of UV filaments suggested an efficient way to increase guided peak intensity in a single UV filament through interference-assisted filament interaction.

As schematically illustrated in Fig. 1(a), the output from a Ti:sapphire amplified laser system (800 nm, ~70 fs, 10 Hz, and ~22 mJ per pulse) was used to generate ~2 mJ third harmonic (TH) pulses through phase-compensated nonlinear frequency-mixing processes.[19] For our experiments, a TH generation efficiency of ~7% was achieved with an output TH pulse of 1.6 mJ. The generated TH pulse was separated from the residual fundamental (FW) pulse with a mirror (high reflection at 267 nm and antireflection at 800 nm), which was then split into two pulses with an energy ratio of 1:1. The two TH pulses were focused by a curve mirror (f=250 mm) to spatially cross in air at a small crossing angle. A motorized stage was used to finely control the time delay. The modulated plasma density was eventually imaged to a charge-coupled device (CCD) after a microscope objective (10×) by recording the emitted fluorescence from the

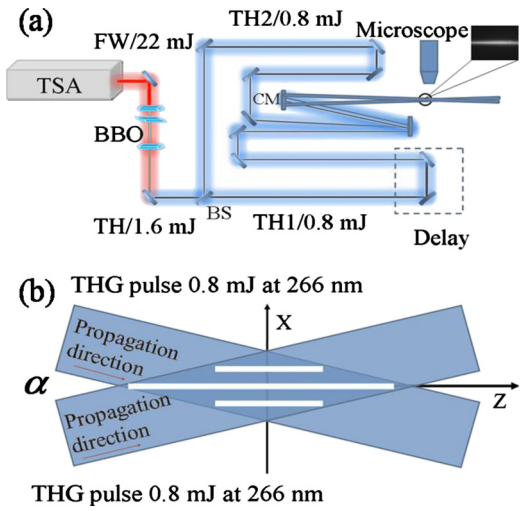

FIG. 1. (Color online) (a) Schematic experimental setup of the interference-assisted interaction of noncollinear UV filaments. BS: beam splitter, CM: curve mirror, And TSA: Ti: sapphire amplifier laser system. (b) Schematic of the magnified area where the two plasma columns overlapped.

[a]Electronic mail: leding@phy.ecnu.edu.cn.

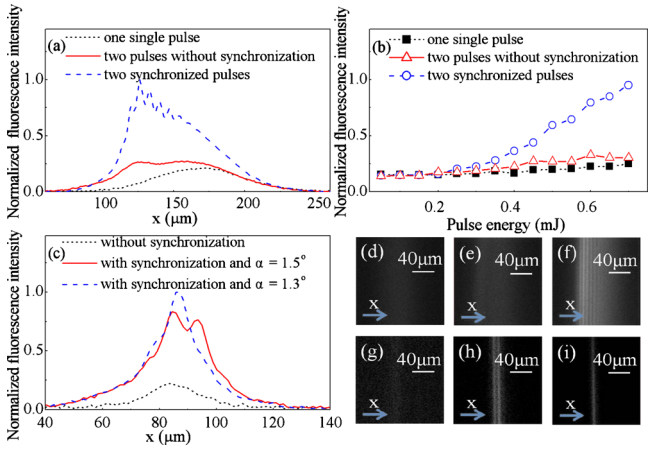

FIG. 2. (Color online) (a) Fluorescence spatial profile of the filament in x direction, and the corresponding images are shown in (d) one single pulse, (e) two pulses without synchronization, and (f) two synchronized pulses with angle of 2.2°. (b) Fluorescence intensity of the plasma grating as a function of the input UV pulse energy. (c) Fluorescence intensity profile of the formed plasma grating and the corresponding images are shown in (g) two pulses without synchronization, (h) two synchronized pulses with angle of 1.5°, and (i) two synchronized pulses with angle of 1.3°, respectively.

ionized molecules inside the interaction region. When the TH pulses were temporally overlapped, the fluorescence intensity increased dramatically, which clearly evidenced plasma grating formation.

Figure 2(a) shows the measured transverse profile of the created plasma grating by the synchronized UV pulses (dashed curve) at a crossing angle of ~2.2°, where the results for the cases without synchronization (solid curve, the time delay between two UV pulses was ~200 fs, and there was no obvious fluorescence intensity enhancement) are also presented for comparison. The dotted curve in Fig. 2(a) stands for the measured fluorescence profile of the filament caused by a single UV pulse. The corresponding two-dimensional spatial images are shown in Figs. 2(d)–2(f), respectively. It is clear that when the plasma grating was formed, the fluorescence intensity was sharply increased. As compared with the IR pulse, the ionization rate is much more significant in the UV domain.[20] The measured molecular fluorescence, which was indicative of the guided field intensity, was significantly increased when the plasma grating was created with respect to the case of single pulse.

We extracted the peak intensity of the recorded fluorescence images inside the plasma grating. Figure 2(b) shows the dependence of the fluorescence intensity on the input energy of the UV pulses. For UV pulse energy from 0.1 to 0.8 mJ, the square-, triangle-, and circular-dotted curves stand for the results by a single UV filament, two UV filaments without synchronization, and two temporally synchronized UV filaments, respectively. As expected for the cases without plasma grating, the fluorescence intensity was almost not changed when the input pulse energy was increased. However, when the plasma grating was formed, the fluorescence intensity increased dramatically as the input UV pulse energy was increased.

Since the formation of photonic crystal filaments was based on the filament interference, the width, and number of self-channels in the overlapped region as well as the period of the formed plasma grating were determined by the interference period $\lambda/[2\sin(\alpha/2)]$,[10] which varied with the crossing angle of the interacting UV pulses. As the crossing angle α was small enough, the interference of the overlapping pulses exhibited a pattern of energy distribution mostly at the center, and the number of the interference fringe decreased with the crossing angle α. As shown in Fig. 2(c), when the crossing angle α was changed slightly from 1.5° to 1.3°, the period was enlarged, and eventually the number of self-channels in the interaction region was reduced to 1, resulting in coalescence of the noncollinear UV fs filaments into an intense single UV filament.

The images of filament caused by one UV pulse was shown in Fig. 2(g), the corresponding measured fluorescence profile was the dotted line in Fig. 2(c). The images of filaments caused by two synchronized pulses at a crossing angle of 1.5° were shown in Fig. 2(h), the corresponding measured fluorescence profile was solid line in Fig. 2(c). It is clear that two single bright filaments were formed for this case. The images of filaments caused by two synchronized pulses at a crossing angle of 1.3° were shown in Fig. 2(i), the corresponding measured fluorescence profile was dashed line in Fig. 2(c). One single bright filament with a diameter of 5 μm was formed as is shown in Fig. 2(i). Please note that full width of half-maximum (FWHM) diameter of the dashed curve in Fig. 2(c) is not so idle, this probably due to a nonparallelism of the CCD pixel array with the filament axis and the integration of the fluorescence signal on many CCD pixel columns, the profile of the plasma filament shown in Fig. 2(c) becomes blur and larger. Although there existed more than one interference fringes in the overlapping region at this crossing angle, the local intensity around the center fringe was much higher than those of side fringes (as the interfering pulses crossed at small angles exhibited nearly Gaussian intensity distribution in the overlapped region). There was only one fringe in the center that underwent filamentation and the other fringes had local intensities insufficient to undergo filamentation. Accordingly, only a single filament was observed with a filament core of quite small diameter.

The solid-dashed curve in Fig. 2(c) shows that each individual UV filament was more than 20 μm in diameter (FWHM), while the coalesced intense single UV filament from the plasma grating exhibited a diameter of ~5 μm, much smaller than the typical diameter of a single IR filament.[21,22] Note that the UV laser could be focused into the limit of $1.22f\,\lambda/D$, where λ is the TH wavelength, $f=250$ mm, and D represents the input beam diameter ($D=9$ mm in our experiment). The width of the induced single filament in the plasma grating obviously went beyond the focusing limitation. As shown in Fig. 2(c), the UV laser-produced plasma could be trapped in a quite small area in comparison with single UV filaments without interference-assisted interaction.

In summary, by using two noncollinearly overlapped UV fs filaments to create wavelength-scale photonic plasma grating, we found that the molecular ion fluorescence was significantly enhanced as compared with that of two filaments without interaction, indicating an increase in the guided field intensity. As the input laser energy rose up, the fluorescence in the overlapped region increased. The period of the plasma grating was dependent on the crossing angle between the interacting filaments and an intense single UV filament could be resulted by finely adjusting a small crossing angle. This may provide an efficient way to control the dynamics of ultraviolet fs filaments, and may stimulate potential applica-

tions with plasma density gratings for high-intensity optics and lattice solitons.[23,24]

This work was partly funded by the National Basic Research Program of China (Grant Nos. 2006CB06001 and 2006CB806005), National Natural Science Fund (Grant Nos. 10525416 and 10804032), and Shanghai Academic Discipline Project (B408).

[1]A. Couairon and A. Mysyrowicz, Phys. Rep. **441**, 47 (2007).
[2]S. L. Chin, " Femtosecond laser filamentation," Laval University, Canada, 2009.
[3]J. Kasparian, M. Rodriguez, G. Méjean, J. Yu, E. Salmon, H. Wille, R. Bourayou, S. Frey, Y. B. André, A. Mysyrowicz, R. Sauerbrey, J. P. Wolf, and L. Wöste, Science **301**, 61 (2003).
[4]R. A. Bartels, T. C. Weinacht, N. Wagner, M. Baertschy, C. H. Greene, M. M. Murnane, and H. C. Kapteyn, Phys. Rev. Lett. **88**, 013903 (2001).
[5]J. Wu, H. Cai, P. Lu, X. Bai, L. Ding, and H. Zeng, Appl. Phys. Lett. **95**, 221502 (2009).
[6]J. Wu, Y. Tong, X. Yang, H. Cai, P. Lu, H. Pan, and H. Zeng, Opt. Lett. **34**, 3211 (2009).
[7]X. Yang, J. Wu, Y. Peng, Y. Tong, S. Yuan, L. Ding, and H. Zeng, Appl. Phys. Lett. **95**, 111103 (2009).
[8]Y. Liu, A. Houard, B. Prade, S. Akturk, and A. Mysyrowiczn, Phys. Rev. Lett. **99**, 135002 (2007).
[9]B. Shim, S. E. Schrauth, C. J. Hensley, L. T. Vuong, P. Hui, A. A. Ishaaya, and A. L. Gaeta, Phys. Rev. A **81**, 061803(R) (2010).
[10]K. Stelmaszczyk, P. Rohwetter, Y. Petit, M. Fechner, J. Kasparian, J.-P. Wolf, and L. Wöste, Phys. Rev. A **79**, 053856 (2009).
[11]D. Majus, V. Jukna, G. Valiulis, and A. Dubietis, Phys. Rev. A **79**, 033843 (2009).
[12]S. Suntsov, D. Abdollahpour, D. G. Papazoglou, and S. Tzortzakis, Appl. Phys. Lett. **94**, 251104 (2009).
[13]X. Yang, J. Wu, Y. Peng, Y. Tong, P. Lu, L. Ding, Z. Xu, and H. Zeng, Opt. Lett. **34**, 3806 (2009).
[14]A. Bernstein, M. McCormick, G. Dyer, J. Sander, and T. Ditmire, Phys. Rev. Lett. **102**, 123902 (2009).
[15]Y. Liu, M. Durand, S. Chen, A. Houard, B. Prade, B. Forestier, and A. Mysyrowicz, Phys. Rev. Lett. **105**, 055003 (2010).
[16]H. Yang, J. Zhang, Y. Li, J. Zhang, Y. Li, Z. Chen, H. Teng, Z. Wei, and Z. Sheng, Phys. Rev. E **66**, 016406 (2002).
[17]P. Kiran, S. Bagchi, S. R. Krishnan, C. L. Arnold, G. R. Kumar, and A. Couairon, Phys. Rev. A **82**, 013805 (2010).
[18]P. Kiran, S. Bagchi, C. Arnold, S. Krishnan, G. Kumar, and A. Couairon, Opt. Express **18**, 21504 (2010).
[19]Y. Wang, X. Dai, J. Wu, L. Ding, and H. Zeng, Appl. Phys. Lett. **96**, 031105 (2010).
[20]A. Couairon and L. Bergé, Phys. Rev. Lett. **88**, 135003 (2002).
[21]J. Wu, H. Cai, Y. Peng, Y. Tong, A. Couairon, and H. Zeng, Laser Phys. **19**, 1759 (2009).
[22]B. Prade, M. Franco, A. Mysyrowicz, A. Couairon, H. Buersing, B. Eberle, M. Krenz, D. Seiffer, and O. Vasseur, Opt. Lett. **31**, 2601 (2006).
[23]J. W. Fleischer, M. Segev, N. K. Efremidis, and D. N. Christodoulides, Nature (London) **422**, 147 (2003).
[24]D. N. Christodoulides and R. I. Joseph, Opt. Lett. **13**, 794 (1988).